Fourier Methods in Tomography, a review

Silvia De Francesco, Augusto Silva

Abstract **– Fourier theory plays a central role in tomography and a special class of reconstruction methods, known as direct Fourier methods, belongs directly from this theory. Recently, related to the demand for 3D reconstruction, the interest for these methods has been growing due to their reduced computational complexity.**

In this paper we are going to review the application of Fourier theory to the field of tomography, both for projection and reconstruction. The basics of direct Fourier methods as well as some specific implementations are addressed.

Resumo **– A teoria de Fourier tem um papel de primeira importância em tomografia e uma classe de metodos de reconstrução, conhecida como métodos directos de Fourier, deriva directamente desta teoria. Recentemente, devido à crescente exigência de reconstrução em 3D, o interesse para estes métodos tem aumentado dada a reduzida complexidade computacional. Neste artigo revê-se a aplicação da teoria de Fourier à tomografia, tanto em reconstrução como em projecção, descrevendo aspectos básicos dos métodos de Fourier assim como algumas específicas implementações.**

Keywords **– Computed tomography, tomographic reconstruction algorithms, direct Fourier methods, sinogram, linogram, rebinning.**

Palavras chave **– Tomografia computorizada, algoritmos de reconstrução tomográfica, métodos directos de Fourier, sinograma, linograma, "rebinning".**

I. Introduction

Given a set of projection data, tomographic reconstruction allows for the visualization of cross sections of an object in a non invasive way. Various reconstruction methods, measurement tools and techniques, have been developed and successfully applied to fields like medicine, astronomy, oceanography, industry etc.

Despite of some peculiarities due to the specific application, tomographic projection and reconstruction processes are based on a common framework in which Fourier theory, with the well known Fourier Slice Theorem (which states the relation between the Fourier transform of parallel projections and the 2D Fourier transform of the object cross section), plays a central role.

Moreover, a special class of reconstruction methods, known as Direct Fourier (or Fourier-based) methods, stems directly from this theory.

The first Fourier-based reconstruction method (applied to astronomy) was described in 1956 by Bracewell [1]. Since then, many Fourier-based methods have been developed, both for projection and reconstruction. With the use of FFT -Fast Fourier Transform- algorithm, Fourier-based reconstruction methods are the fastest now available being preferred in data intensive applications like *microtomography* [2], and suitable for 3D reconstruction. In fact, compared with the Filtered Backprojection –FBP– method which has a computational complexity of $O(N^3)$, the computational complexity of the direct Fourier methods is about $O(N^2 \log N)$. Moreover, also from the point of view of image quality, direct Fourier methods are now able to compete with methods like filtered backprojection.

Although Fourier methods applied to 3D reconstruction have been recently described [3], this paper will concern only with 2D tomography, meaning that both projection and reconstruction processes are limited to a plane (section) transversal to the object being studied.

In section II the basics of tomography are briefly described, a complete and rigorous approach to this field can be found in [4], [5] and [6].

Section III deals with the standard direct Fourier method, which suffers from distortion, and with some of the most significant implementations aiming to solve the distortion problem through different sampling-interpolation schemes.

Fourier methods are not directly suitable for divergent projections, this means that in order to be applied to the real data (which normally are taken with divergent geometry) a rebinning step has to be performed. This procedure, as well as some comments about the possible development of a Fourier method to be directly applied to divergent projections, is described in section IV.

In section V, the Fourier based projection process is briefly described and, finally, in section VI a few results are shown, comparing the quality of the reconstructed images.

II. Basics of tomography

Some physical phenomena can be modeled, from a mathematical point of view, as the calculation of a line integral of some physical parameter along straight lines. For instance in Computer Tomography –CT–, the intensity of an x-ray traveling through a body suffers an attenuation that can be modeled as the integral of attenuation coefficient of the tissues calculated along

the line from focus to detector.

The distribution of a parameter on a transversal section of an object is described by a 2D function f (object function) in the (x, y) plane of the section. In most of the applications (medical, for example), the function f is limited in space, which means that it vanishes outside a finite region of the plane. An important consequence of this characteristic (we'll see how it affects Fourier reconstruction methods) is that the 2D Fourier transform of an object function is not band limited.

The two parameters θ (slope of the line $+\frac{\pi}{2}$) and s (distance to the center of rotation) univocally specify the line with equation

$$x\cos\theta + y\sin\theta = s \tag{1}$$

in the (x, y) plane and the general formula for the line integral, known as the Radon transform of $f(x, y)$, is:

$$p(\theta, s) = \iint f(x, y)\delta(x\cos\theta + y\sin\theta - s)dxdy \tag{2}$$

A projection consists of a collection of integrated values of $f(x, y)$ taken along a set of straight lines in the plane and the projection data set is given by a number of projections taken with different orientations. Basically, two geometries have been defined for the sets of line integrals making a 2D projection: parallel and divergent (or fan-beam).

In parallel geometry (historically, the first to be used), a projection $p_\theta(s)$ consists of a collection of line integrals (2) taken along straight parallel lines in the plane, that means, a collection of $p(\theta, s)$ with constant θ (fig. 1) and $s \in \left[-\frac{S}{2}, \frac{S}{2}\right]$.

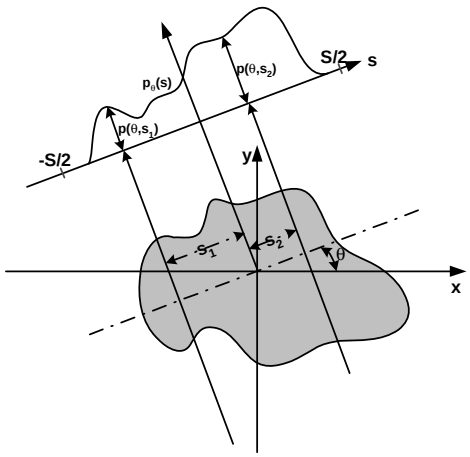

Figura 1 - An object $f(x, y)$ and its paralel projection $p_\theta(s)$.

In divergent geometry, to each angular position of the focus corresponds a fan of focus-detector lines (the detector being an array of detector elements). In this case, each line is defined by a pair of parameters (β, γ), where β is the slope of the central line of the beam $+\frac{\pi}{2}$ and γ is the angular offset of the line relative to the central one (fig. 2). Being Γ the fan-angle and r the focus-center of rotation distance, the equation of the line is

$$x\cos(\beta+\gamma) + y\sin(\beta+\gamma) = -r\sin\gamma \tag{3}$$

and each divergent projection is described by the formula:

$$\begin{aligned} p_\beta(\gamma) \quad = \quad & \iint f(x, y)\delta(x\cos(\beta+\gamma) + \\ & y\sin(\beta+\gamma) + r\sin\gamma)dxdy \end{aligned} \tag{4}$$

with constant β and $\gamma \in \left[-\frac{\Gamma}{2}, \frac{\Gamma}{2}\right]$.

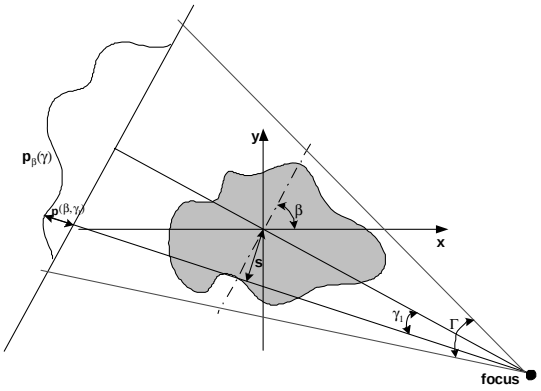

Figura 2 - An object $f(x, y)$ and its fan-beam projection $p_\beta(\gamma)$.

In Radon space (θ, s), the space of $f(x, y)$ Radon transform, a projection data set for a given geometry corresponds to a set of samples taken over a specific sampling grid. A projection data set for parallel geometry, called sinogram, is a 2D matrix (fig. 3a) where to each row corresponds a value for the parameter θ (a parallel projection), and to each column a value for the parameter s.

Similarly, a projection data set for a divergent geometry is a 2D matrix (fig. 3-b) where to each row corresponds a value for the parameter β (a divergent projection) and to each column a value for the parameter γ.

Figure 3 turns easy to understand that, given a divergent projections data set, it's possible to evaluate an approximation of a sinogram rearranging and interpolating the samples to the new grid. This process, called rebinning (section IV-A), allows us to apply to divergent projections data sets the reconstruction methods that are suitable only to sinograms.

A. Fourier Slice Theorem

The Fourier slice theorem (see [4] for details and demonstration) states that:

Theorem 1: The Fourier transform of a parallel projection of an object function $f(x, y)$ taken at angle θ gives a slice of the two dimensional transform of $f(x, y)$, $F(u, v)$, subtending an angle θ with the u axis.

In other words, the 1D Fourier transform $P_\theta(\sigma)$ of the parallel projection $p_\theta(s)$, gives the values of $F(u, v)$ along line BB in figure 4.

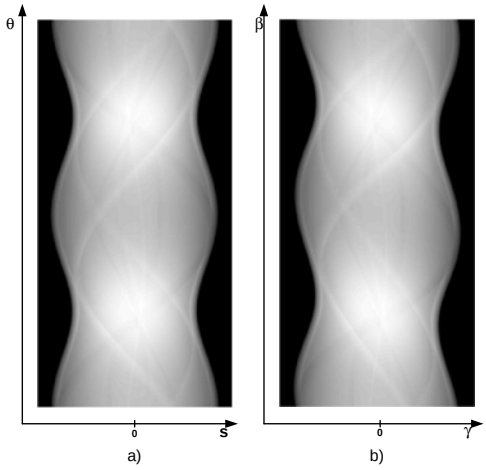

Figura 3 - Projection data sets of Herman head phantom for parallel and divergent geometries: a) sinogram (512 projections over 360^o, 255 rays); b) divergent projections data set (512 projections over 360^o, 255 rays).

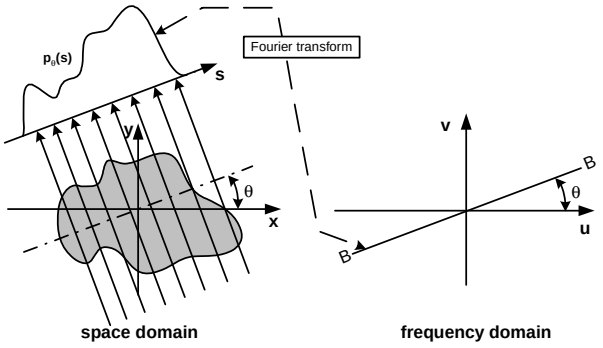

Figura 4 - Graphic visualization of Fourier slice theorem statement.

III. Fourier reconstruction methods for parallel projections

The Fourier slice theorem suggests a simple way to solve the reconstruction problem. Taking parallel projections of the object function f at angles θ_1,θ_2,...θ_n and Fourier transforming each of them, we obtain the 2D Fourier transform of the object function $F(u, v)$ on n radial lines like in figure 5. In ideal conditions (infinite number of projections and samples per projection) $F(u, v)$ would be known at all points in the frequency domain and the object function $f(x, y)$ could be recovered by 2D inverse Fourier transforming $F(u, v)$.

Fourier reconstruction methods (also known as direct Fourier or Fourier based methods) follow directly from this ideal procedure, adapted to the discrete case.

In practice, only a finite number of projections and samples per projection are taken and $F(u, v)$ is known just on a finite number of points along a finite number of radial lines and, in order to obtain an approximation of $f(x, y)$ by 2D inverse Fourier transform of $F(u, v)$, we have to interpolate from the radial points to the points on a Cartesian grid. Basically, Fourier reconstruction methods are three steps methods:

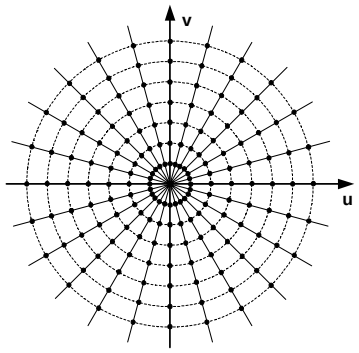

Figura 5 - Fourier transform of parallel projections gives samples of the 2D Fourier transform of the object along radial lines.

- 1D discrete Fourier transform (through FFT algorithm) of the parallel projections taken at n angles θ_1,θ_2,...θ_n
- Polar to Cartesian grid interpolation
- 2D inverse Fourier transform (again, using FFT).

Avoiding theoretical aspects that exceed the aim of this paper, we'll make some comments about potential sources of error and refinements that can be introduced in Fourier reconstruction methods (in general) in order to improve the performance [7].

From sampling theory, we know that the number of projections over 180^oshould be larger than the essential bandwidth of the image b (rad/length unit) and that the distance between samples (for parallel projections) should be less or equal to π/b [5]. This gives us a theoretical lower bound for the number of samples per projection. Anyway, it's common practice to take a number of projections M approximately twice the number of pixels N in the x and y directions of the image, and N samples per projections (which is a sufficient number of samples). The problem is that a physical object is virtually unlimited in frequency and, even if we collect a number of samples according to the lower bound, aliasing in the Fourier domain may still occur. In order to reduce this phenomenon a technique, called "zero-padding", can be introduced. This technique consists in adding zeros to each end of the projection signal before transforming. The transformed signal has a double sample density and the periodical repetitions of the spectrum pattern are moved apart reducing the aliasing effect. In 2D Fourier domain, the polar to Cartesian grid interpolation is performed over the denser domain and, after 2D inverse Fourier transform, the image is recovered keeping just the central part of the result.

Eventually, undersampling of the Fourier domain gives rise to aliasing in the space domain after inverse 2D Fourier transforming. In this case, a technique called "gridding" can be applied to the polar to Cartesian grid interpolation step. This technique consists in interpolating to a finer Cartesian grid, for instance, doubling the number of points in the u and v directions (which means quadruplicating the total number

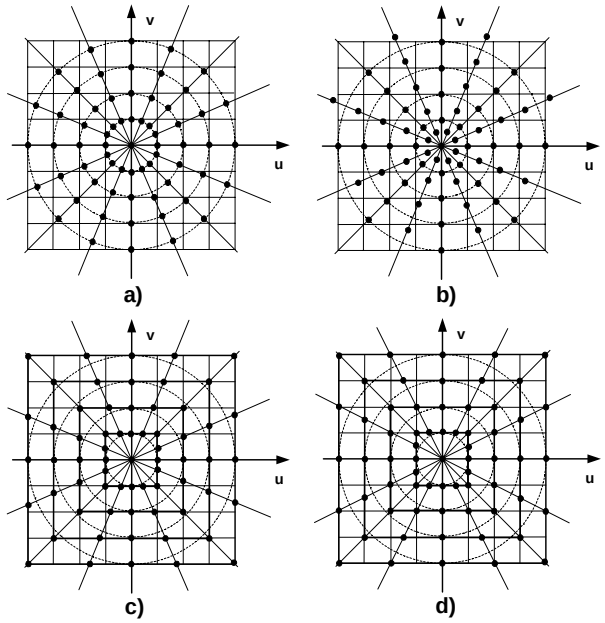

Figura 6 - Examples of polar and Cartesian grids for interpolation. a) Conventional polar and Cartesian grids. b) Modified polar grid with a radial offset of the samples at alternate angles. c) Modified polar square grid with samples calculated at intersections with concentric squares. d) Modified polar grid for linogram projections.

of points). Also in this case, after 2D inverse Fourier transform, the image is recovered keeping just the central part of the result.

While improving image quality, the former techniques deteriorate the computational performance of the algorithm because of the larger number of data involved.

Certainly, the most critical step is the polar to Cartesian grid interpolation in Fourier domain and most of the existing Fourier reconstruction methods basically differ just on the way they deal with the interpolation step.

A. Polar to cartesian grid interpolation

Comparing the polar and the Cartesian grids in figure 6-a, it becomes clear that the polar grid is a very inefficient way to sample the Fourier domain. The fact that, close to the origin (where most of the frequency information is concentrated), the polar samples are separated by a very short angular distance and by a long radial distance, has suggested that a trade off should be found between the unnecessary fine angular sampling and the unsufficient radial sampling.

First of all, while linear interpolation in the angular direction is normally acceptable, in the radial direction a higher order filter should be used. For example, a method proposed by Low and Natterer [8] uses nearest neighbour interpolation in the angular direction and a modified sinc interpolation filter applied to the sample set with double density in the radial direction (obtained by zero-padding of the sinogram).

In any case, whatever the method choosed for interpolation, since the density of the points in the polar grid becomes sparcer far away from the center, the interpolation error increases at higher frequencies.

Some authors have introduced modifications to the starting polar grid leading to faster and/or more accurate interpolation:

A.1 Polar interleaved grids

Lewitt, in [7], asserts that the performance of Fourier reconstruction algorithm can be improved by interleaving two polar sample grids in Fourier space like in figure 6-b. Such a pattern can be obtained by offsetting the samples from alternate projections, this means that the 1D Fourier transform of (let's say) even projections has to be computed in points shifted of half a radial sample increment relative to the odd projections.

This way, the average distance between samples is considerably reduced and an even better result can be obtained by applying techniques like zero padding of the projections.

A.2 Concentric squares grid

This sampling pattern can be obtained by varying the distance between consecutive projection rays with a factor of $\cos\theta$ for projection angle $\theta \in [-45^o, 45^o)$ and $\sin\theta$ for projection angle $\theta \in [45^o, 135^o)$. The effect in the Fourier domain can be seen in figure 6-c where the sample points are distributed over a polar-squared grid. The same effect in Fourier domain can be obtained with a conventional parallel projection set by chirp-z transforming each projection with the desired distance instead of 1D Fourier transforming.

The advantage of this sample pattern due to Pasciak [8] is that the interpolation step in the Fourier domain can be performed just in one dimension: on vertical lines for angles between -45^o and 45^o and on horizontal lines for angles between 45^o and 135^o.

B. Other methods

Some methods have been conceived in order to completely avoid the interpolation step in the Fourier space.

B.1 Linogram

This method (see [9] for a detailed and rigorous description) is based on the so called linogram projections which are taken varying the distance between consecutive projection rays with a factor $\cos\theta$ for $\theta \in [-45^o, 45^o)$ and $\sin\theta$ for $\theta \in [45^o, 135^o)$. Moreover the projection angles are not taken in equidistant θ steps but in equidistant $\tan\theta$-steps for $\theta \in [-45^o, 45^o)$ and equidistant $\cot\theta$-steps for $\theta \in [45^o, 135^o)$. After 1D Fourier transform of the projections, the sampling pattern in the Fourier domain appears like in figure 6-d, with half of the points evenly spaced along radial and vertical lines and the other half of the points evenly spaced along radial and horizontal lines. This pattern looks similar to the pattern of figure 6-c with the difference that the samples are unevenly distributed in the angular direction and because of this cannot

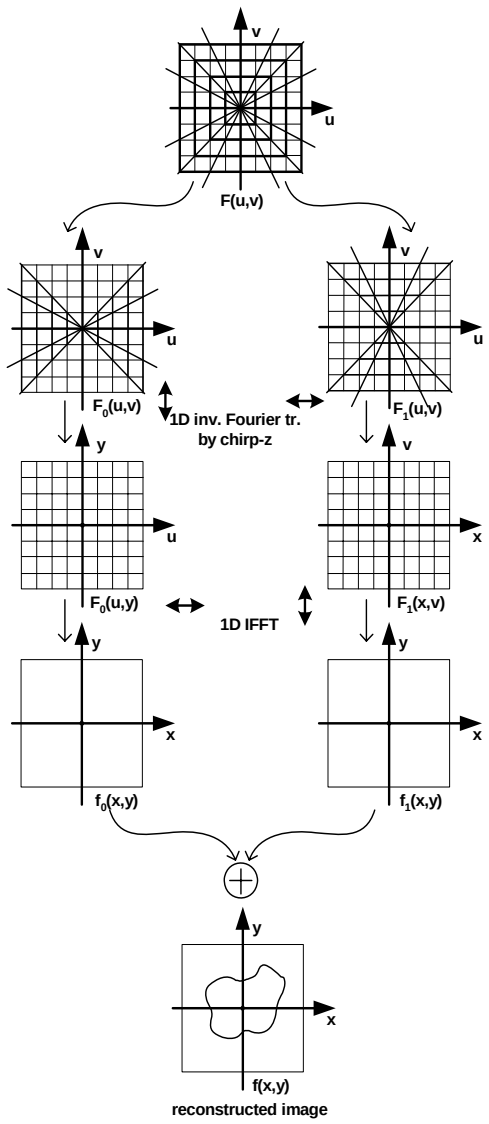

Figura 7 - Flow diagram of the Linogram direct Fourier method starting by the Fourier domain decomposition step.

be obtained by simple chirp-z transform of the conventional parallel data set like in that case. In this case a process called rebinning (section IV-A) should be applied.

The Linogram direct Fourier method proceeds with the decomposition of Fourier sample data in two subspaces F_0 and F_1, corresponding to the projection angles included in $\theta \in [-45^o, 45^o)$ and $\theta \in [45^o, 135^o)$, which are kept separated until the last step of the algorithm (fig. 7). For F_0 the first inverse Fourier transform is computed in the vertical direction (by chirp-z transform) and the second in the horizontal direction (by simple FFT), while for F_1 the first inverse Fourier transform is computed in the horizontal direction (by chirp-z transform) and the second in the vertical direction (by simple FFT). Finally, the two functions f_0 and f_1 are added obtaining the reconstructed image.

It has to be noticed that the use of the chirp-z transform, which can handle different equidistant data spacing, avoids any interpolation in the Fourier domain.

B.2 NUFFT-based methods

Some new algorithms have been proposed based on recent developments connected to the efficient computation of discrete Fourier transform for non-equispaced data (NUFFT - Non Uniform Fast Fourier Transform [10] [11] [12]).

These algorithms are designed for different sampling geometries in the Fourier domain of the image and allow to perform the reconstruction completely avoiding the interpolation step. For instance in [13] and [14] the algorithm basically flows in two steps: first the 1D FFT of the projections is calculated with a given oversampling factor obtaining a conventional oversampled polar grid and then 2D inverse NUFFT is applied directly to this sample pattern.

Again in [13] another algorithm based on the linogram geometry is described (in this case the author identifies as linogram geometry the geometry of figure 6-c). The algorithm flows exactly like the one of figure 7, with the difference that, since the samples in the Fourier domain are not equispaced in the vertical nor in the horizontal directions, the 1D inverse Fourier transform is performed through NUFFT instead of chirp-z transform.

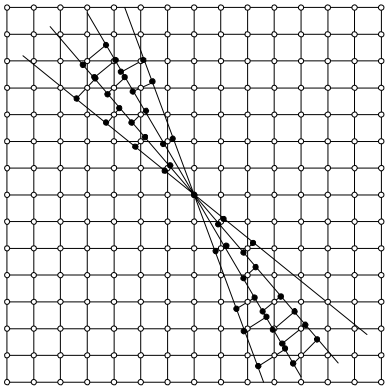

Figura 8 - The interpolation scheme proposed by Fourmont

An original approach, due to Fourmont [14], is based on a pre-computation step in which a sample pattern is determined, suitable for interpolation just in the angular direction (in this case linear interpolation suffices). In order to obtain such a sampling pattern (figure 8), for each point p of the Cartesian grid to be evaluated, the two closest radial segments in the angularly discretized polar coordinate system are determined and, on these segments, the points (the black dots) having the same radial coordinate than p. For each projection, the Fourier transform is calculated through 1D NUFFT in those points and then the samples on the Cartesian grid are calculated by linear interpolation in the angular direction of the associated couples of points with pre-calculated (in the pre-computation step) interpolation coefficient. The last step of the algorithm is, of course, the 2D inverse FFT.

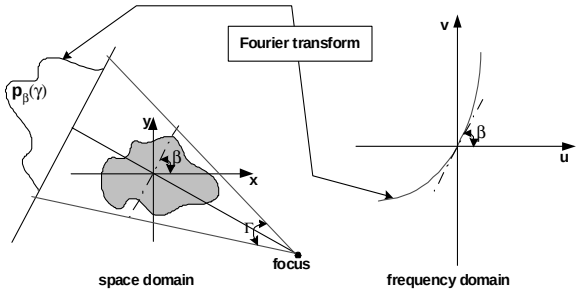

Figura 9 - Adaptation of Fourier slice theorem to a divergent projection.

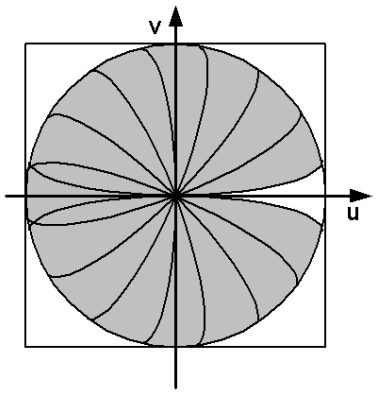

Figura 10 - Sample pattern for divergent beam projections data in the Fourier domain.

B.3 Fourier Series Method

In this method, which uses conventional parallel projections and is described by Gottlieb in [15], the interpolation in Fourier space is avoided by relating (again, based on the slice theorem) the Fourier series of $p_\theta(s)$ to the truncated Fourier series of the image function. In this case, an analytical formula for the exact evaluation of the Fourier coefficients of $f(x, y)$ in terms of the Fourier coefficients of $p_\theta(s)$ is derived and implemented with some approximation (truncation of infinite terms sums). From the point of view of image quality, the results of this method are similar to those obtained with filtered backprojection method.

IV. Fourier reconstruction methods for divergent projections

Unfortunately, since Fourier slice theorem applies just to parallel projections, the classical Fourier reconstruction methods don't match the case of divergent geometry. In figure 9 we show a graphic representation of Fourier slice theorem adapted to divergent projections: the Fourier transform of a divergent projection taken at angle θ gives, in the frequency space, n points along a curve described (in polar coordinates (θ, s)) by the equation

$$\theta = \beta - \arcsin\frac{s}{r} \tag{5}$$

giving rise to the sample pattern of figure 10.

An interesting remark concerning whatever reconstruction method for divergent projections is that, while in the parallel case projections have to be taken over an arc of just 180^o in order to cover the complete Fourier domain, in the divergent case a larger arc has to be considered. Namely, an arc of $180^o + \Gamma$ is the minimum arc to be considered. This well known fact can also be seen in the frequency sample pattern of figure 10 where, intentionally, have been drawn just projections with $\beta \in [0, 180^o]$ and the unshaded sector of Fourier domain results uncovered.

Intuitively, one can imagine three possible ways to apply Fourier reconstruction methods to divergent projections. The first way is to interpolate parallel projection data from divergent projection data and then simply apply a classical Fourier reconstruction method. The interpolation process performed in the projections domain is called rebinning and will be described below.

The second is to interpolate in the frequency domain from the sample pattern of figure 10 to a cartesian grid and then 2D inverse Fourier transform like in classical methods.

The last is to develop a Fourier reconstruction method to be applied directly to the divergent data set.

To our knowledge, the second and the third way are still unattempted, probably due to the difficulties in the interpolation step. Nevertheless, taking advantage of recent development in NUFFT calculation, an attempt should be made in order to inverse Fourier transform based on such a sampling grid.

A. Rebinning

We'll describe here the most straightforward type of rebinning that allows to obtain parallel data sets from divergent ones. Anyway, has to be pointed out that rebinning in general can be applyed also to obtain linogram and other geometries' data sets from divergent or parallel ones [9] (and vice-versa, even if it is not useful from a practical point of view).

Rebinning is a well known interpolation process that has been employed in the first divergent beam CT scanners until the advent of reconstruction methods dedicated to that geometry (fan beam filtered backprojection). Since interpolation is performed in the projection domain, it is not a critical operation like it is in the Fourier domain and can even be performed linearly without introducing noticeable error.

Comparing equations 1 and 3, we see that the parameters of a ray in the parallel geometry are related to the parameters of the corresponding ray in the divergent geometry by the simple equations:

$$\beta = \theta - \gamma \tag{6}$$

$$\gamma = -\arcsin\frac{s}{r}. \tag{7}$$

Thus, to each sinogram sample to be computed corresponds a point in the space of the divergent projections which value can be evaluated through interpolation.

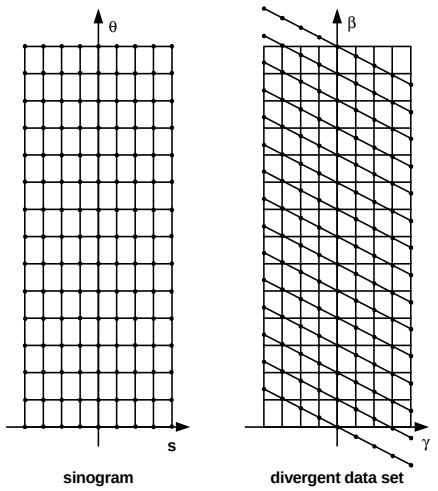

Figura 11 - Rebinning process: dots represent the desired sinogram sample points and the corresponding interpolated points in the divergent projections space.

It's interesting to notice that to a line of sinogram samples corresponds a line of points slanted -45^o in the divergent projections space (figure 11), fact that can be also observed in figure 3.

To confirm the remark made about the minimum amplitude of the rotation arc for a complete set of divergent projections, can be observed that, in order to obtain a complete sinogram for $\theta \in [0, 180^o]$, at least divergent projections with $\beta \in [-\Gamma/2, 180^o + \Gamma/2]$ has to be known.

V. Fourier projection method

Direct Fourier method can also be applied in the reverse order allowing for the calculation of projection data sets from a digital sample object. Thus, the Fourier projection method flows in three steps:

- 2D Fourier transform (through FFT)
- Cartesian to polar interpolation
- 1D discrete inverse Fourier transform (through FFT algorithm) of the radial segments od the polar grid obtaining the parallel projections.

Despite of the usual problems due to interpolation in the Fourier domain, Fourier projection method (which is very fast) has been used in iterative reconstruction methods in order to speed up the reprojection step. Approaches similar to those described for the reconstruction methods can be used in order to reduce the interpolation error.

Recently, Fessler has described a new Fourier based iterative method using min-max interpolation for the NUFFT, both in projection and in backprojection steps, obtaining an efficient iterative approach to the reconstruction problem [16].

In any case, it has to be pointed out that here the interpolation step is not so critical as in the reconstruction methods since the sample points in the starting grid (Cartesian) are uniformly distributed.

VI. Some examples

In order to have an idea of the effectiveness of the described algorithms, when compared with the commonly used FBP algorithm, we've performed some simulations using the Herman head phantom [17] as a model of an object's transversal section (fig. 12).

Figura 12 - Herman head phantom.

The simulator, both projection and reconstruction processes, has been implemented in Matlab and the reconstruction error has been quantitatively evaluated measuring the distance between the original and the reconstructed images. For this purpose we've used the distance metrics proposed by Herman [17] (d- normalized root mean squared distance, r- normalized mean absolute distance, e- worst case distance measure) applied to the region of interest of the images.

In figure 13 are shown some images obtained with different reconstruction methods applied on the same parallel projection data set and in table I are summarized the results of the reconstruction error evaluation. At a first glance it's clear that the quality of the DFM with simple two dimensional linear interpolation in the Fourier space is unacceptable but it significantly improves introducing zero padding of the projections. Moreover, with the introduction of two dimensional cubic interpolation in the Fourier space an even better result is obtained, comparable to the result obtained through FBP. The behaviour of the different methods can be grafically evaluated in figure 14 where the diagonal profile of the reconstructed images and of the original one are compared. Also in this case the good quality of the DFM with zero padding and cubic interpolation in the Fourier domain is confirmed.

The last column of table I summarizes the reconstruction time of the different methods and shows how Fourier based methods are impressively faster than the commonly used FBP method.

The results obtained with the corresponding reconstruction methods applied to the divergent projection data set are shown in figure 15 and compared in table II. In this case the FBP is applied directly to the divergent beam data set (DBFBP stands for "divergent beam filtered backprojection") while the Fourier based methods are preceded by a rebinning step and

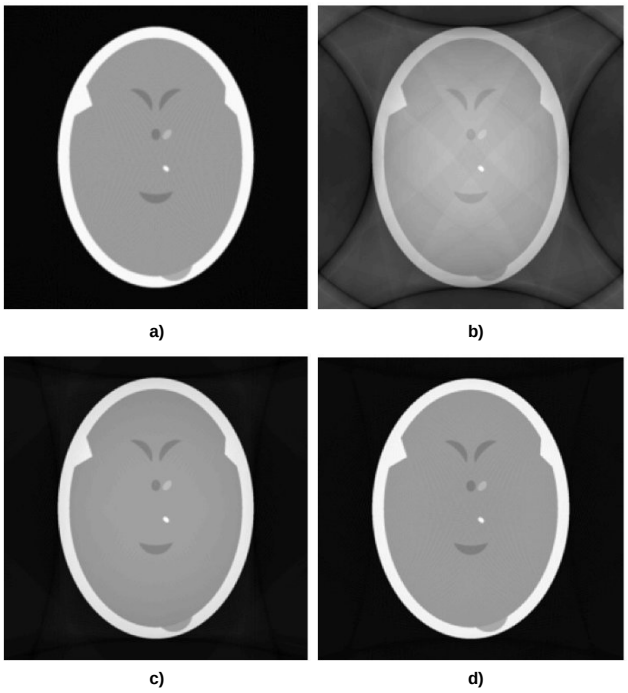

Figura 13 - Images obtained with different reconstruction methods from parallel projection data set: a) filtered backprojection; b) direct Fourier method with linear interpolation in the Fourier space; c) direct Fourier method with zero padding of the projections and linear interpolation in the Fourier space; d) direct Fourier method with zero padding of the projections and cubic interpolation in the Fourier space.

are applied on the synthesized parallel projection data set. From the perceptual point of view the obtained images do not show any remarkable difference with respect to those of figure 13. The quantitative evaluation of the reconstruction error does confirm the perceptual analysis, showing that the rebinning step, prior to reconstruction, doesn't affect image quality. The only item that differs from the corresponding in the parallel beam case is the reconstruction time which increment, in the case of Fourier based methods, corresponds to the rebinning time while, in the DBFBP case, is due to the larger amount of data to be processed (our implementation of DBFBP, which considers all the views corresponding to a 360^orotation of the focus, can be improved considering just the views corresponding to $180^o + \Gamma$ rotation of the focus). Also in this case, the Fourier based methods show an impressive reduction of reconstruction time.

VII. Conclusions

Far from the goal of having completely covered the subject, we've given an overview of the main topics of Fourier reconstruction methods. A number of implementations have been described and some important aspects have been pointed out. Topics like iterative Fourier based algorithms have been just touched and other like 3D Fourier reconstruction have been left for further pubblications.

The results of the performed simulations have been

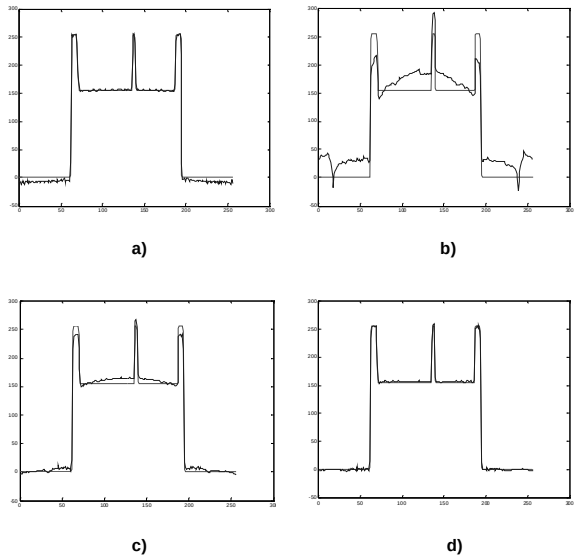

Figura 14 - Comparison between the diagonal of the original image (fig. 12) and the diagonals of the reconstructed ones (fig. 13). a) original to FBP. b) original to DFM. c) original to DFM with zero padding. d) original to DFM with zero padding and cubic interpolation in the Fourier space.

analysed qualitatively and quantitatively showing that direct Fourier reconstruction methods are a valid alternative to the commonly used FBP algorithm with a remarkable reduction in computation time.

VIII. Acknowledgement

This work is being financially supported by *FCT - Fundação para a Ciência e Tecnologia-*.

Referências

[1] R. N. Bracewell, "Strip integration in radio astronomy", *Australian J. Phys.*, vol. 9, pp. 198–217, 1956.

[2] B. Fornberg and B. Herbst, "Modeling in applied mathematics", Lectures notes for the "Image Processing" course, University of Stellenbosch, Department of Applied Mathematics, May 2000.

[3] S. Schaller, T. Flohr, and P. Steffen, "An efficient Fourier method for 3-D Radon inversion in exact cone-beam CT reconstruction", *IEEE Trans. on Med. Imaging*, vol. 17, no. 2, pp. 244–250, 1998.

[4] A. C. Kak and M. Slaney, *Principles of Computerized Tomographic Imaging*, IEEE Press, 1988.

[5] F. Natterer, *The Mathematics of Computerized Tomography*, Wiley, J., 1986.

[6] F. Natterer and F. Wubbeling, *Mathematical Methods in image reconstruction*, SIAM Monographs on Mathematical Modeling and Computation. SIAM, Society for Industrial and Applied Mathematics, Philadelphia, 2001.

[7] R. M. Lewitt, "Reconstruction algorithms: transform methods", *Proceedings of the IEEE*, vol. 71, no. 3, pp. 390–408, 1983.

[8] F. Natterer, "Fourier reconstruction in tomography", *Numer. Math.*, vol. 47, pp. 343–353, 1985.

Method \ Distance measure	d	r	e	time (sec.)
FBP (Ram-Lak filter)	0.0341	0.0109	16.0662	39.0160
DFM linear int.	0.2602	0.1494	127.9453	0.8610
DFM z. pad. linear int.	0.0772	0.0439	35.5385	2.9740
DFM z. pad. cubic int.	0.0249	0.0125	11.8202	6.0790

Tabela I

Quality of images reconstructed from parallel projection data set (fig. 13).

Method \ Distance measure	d	r	e	time (sec.)
DBFBP (Ram-Lak filter)	0.0342	0.0108	15.5640	187.2680
DFM linear int. (*)	0.2616	0.1498	127.6399	1.9230
DFM z. pad. linear int. (*)	0.0805	0.0448	35.5215	3.0870
DFM z. pad. cubic int. (*)	0.0324	0.0141	14.3563	7.2110

Tabela II

Quality of images reconstructed from divergent projection data set (fig. 15). (*) Including rebinning step.

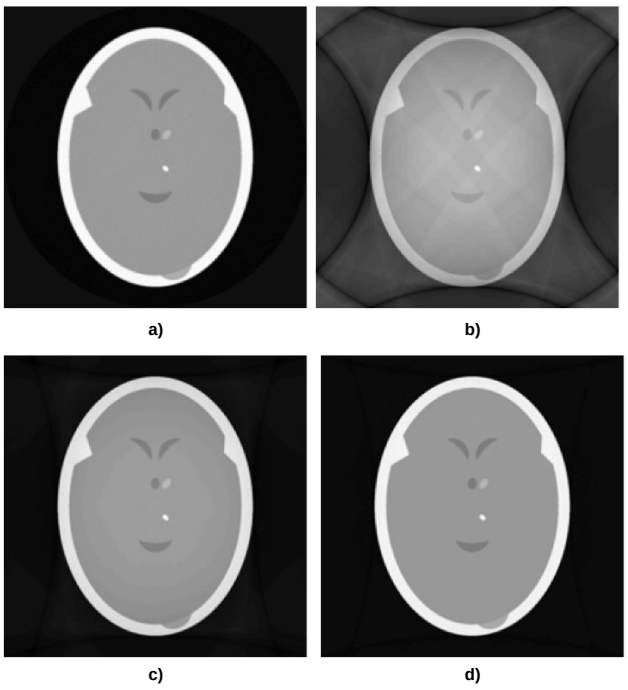

Figura 15 - Images obtained with different reconstruction methods from divergent projection data set: a) filtered backprojection; b) direct Fourier method with linear interpolation in the Fourier space; c) direct Fourier method with zero padding of the projections and linear interpolation in the Fourier space; d) direct Fourier method with zero padding of the projections and cubic interpolation in the Fourier space.

[9] M. Magnusson, *Linogram ad other direct Fourier methods for tomographic reconstruction*, Phd, University of Linköping, 1993.

[10] A. Dutt and V. Rokhlin, "Fast Fourier transforms for nonequispaced data", *SIAM J. Sci. Comput.*, vol. 14, no. 6, pp. 1368–1393, 1993.

[11] A. F. Ware, "Fast approximate Fourier transforms for irregularly spaced data", *SIAM Rev.*, vol. 40, no. 4, pp. 838–856, 1998.

[12] D. Potts, G. Steidl, and M. Tasche, "Fast Fourier transforms for nonequispaced data: a tutorial", in *Modern sampling theory: mathematics and applications*, J. J. Benedetto and P. J. S. G. Ferreira, Eds., Applied and Numerical Harmonic Analysis Series, pp. 249–274. Birkhauser, Boston, 2001.

[13] D. Potts and G. Steidl, "New Fourier reconstruction algorithms for computerized tomography", in *SPIE's International Symposium on Optical Science and Technology: Wavelet Applications in Signal and Image Processing VII*, A. Aldroubi, A. F. Laine, and M. A. Unser, Eds., S. Diego (CA), 2000, vol. 4119, pp. 13–23, SPIE.

[14] K. Fourmont, "Non-equispaced fast Fourier transforms with applications to tomography", *pre-print*, 2000.

[15] D. Gottlieb, B. Gustafsson, and P. Forssén, "On the direct Fourier method for computed tomography", *IEEE Trans. on Med. Imaging*, vol. 19, no. 3, pp. 223–232, 2000.

[16] J. A. Fessler and B. P. Sutton, "Nonuniform Fast Fourier transforms using min-max interpolation", *IEEE Trans. on Signal Processing*, vol. Submitted, 2001.

[17] G. T. Herman, *Image Reconstruction from Projections*, Academic Press, 1980.